MORPHOLOGICAL ASSESSMENT OF APOPTOSIS AND NECROSIS SIGNS IN THE GASTRIC MUCOSA IN A MODEL OF HEPATORENAL SYNDROME

Sanjar F. Allaberganov - independent researcher
Urgench State Medical Institute (Urgench, Uzbekistan)
Dilorom B. Adilbekova - professor
Abdulaziz A. Akhrorov - student
Tashkent State Medical University (Tashkent, Uzbekistan)
zebooriginal@gmail.com

Abstract. Introduction: *Hepatorenal syndrome (HRS) is a severe complication of end-stage liver disease characterized by functional renal failure and accompanied by pronounced systemic and splanchnic hemodynamic disturbances. The impact of HRS on the integrity of the gastric mucosa, particularly the balance between apoptosis and necrosis of cells, remains insufficiently studied, although it has important clinical significance for assessing the risk of gastrointestinal bleeding.*

Objective: *To perform a detailed morphological and quantitative assessment of apoptosis and necrosis markers in the gastric mucosa using an experimental model of HRS.*

Materials and methods*: The study was conducted at the clinics of Tashkent State Medical University. HRS was modeled in 60 male Wistar rats using a two-stage protocol: common bile duct ligation (BDL) to induce secondary biliary cirrhosis, followed by a single intraperitoneal injection of carbon tetrachloride (CCl_4) to provoke acute-on-chronic liver failure and subsequent renal dysfunction. The animals were divided into three groups: Sham operation (n=20), cirrhosis (n=20), and HRS (n=20). Gastric mucosal samples were collected on day 28. Morphological evaluation was performed using hematoxylin–eosin (H&E) staining to identify necrotic changes and the TUNEL (terminal deoxynucleotidyl transferase dUTP nick end labeling) assay to detect apoptosis. Immunohistochemical expression of cleaved caspase-3, Bax, and Bcl-2 was also assessed.*

Results: *The HRS group demonstrated significantly more severe gastric mucosal injury compared with the cirrhosis group without HRS. The mean apoptosis index (TUNEL-positive cells per field) was 4.2±1.1 in the Sham group, 18.5±3.4 in the cirrhosis group, and reached 34.7±5.2 in the HRS group ($p<0.01$). Foci of coagulative necrosis were observed in 75% of HRS samples and only in 20% of cirrhosis samples. Immunohistochemical analysis revealed significant activation of the pro-apoptotic markers Bax and cleaved caspase-3, along with a decrease in the anti-apoptotic marker Bcl-2 in the HRS group, resulting in a shift of the Bax/Bcl-2 ratio toward apoptosis.*

Conclusion: *The development of HRS on the background of cirrhosis aggravates gastric mucosal injury, leading to a high level of both apoptotic and necrotic cell death. These findings suggest that the hemodynamic and metabolic disturbances characteristic of HRS create an unfavorable microenvironment in the gastric mucosa, promoting a mixed type of cell death that may contribute to an increased risk of erosions and gastrointestinal bleeding in such patients.*

Keywords: *Hepatorenal syndrome, gastric mucosa, apoptosis, necrosis, TUNEL assay, morphology, experimental model, caspase-3.*

Introduction. Hepatorenal syndrome (HRS) is a life-threatening complication of progressive cirrhosis and is defined by the International Ascites Club as a functional and potentially reversible form of renal failure that develops in the setting of severe hepatic insufficiency and portal hypertension. The pathophysiology of HRS is complex and multifactorial, primarily driven by pronounced splanchnic vasodilation, which leads to a reduction in the effective arterial blood volume. This, in turn, activates powerful vasoconstrictor systems, including the renin–angiotensin–aldosterone system (RAAS), the sympathetic nervous system (SNS), and the release of vasopressin,

ultimately resulting in intense renal vasoconstriction and a marked decrease in the glomerular filtration rate (GFR). Although renal dysfunction is the defining feature of HRS, the systemic and splanchnic hemodynamic disturbances characteristic of this condition exert widespread effects on other organs, including the gastrointestinal tract.

The gastric mucosa is particularly vulnerable to hypoperfusion and ischemia. In cirrhosis and portal hypertension, the gastric mucosa is already compromised, a condition commonly referred to as portal hypertensive gastropathy (PHG). PHG is characterized by dilated and tortuous submucosal vessels, reduced effective mucosal blood flow despite increased overall gastric blood flow, and increased susceptibility to injury from various toxic agents. A study by Zhang et al. (2023) significantly advanced the understanding of the molecular mechanisms of gastric injury in portal hypertension by demonstrating marked activation of hypoxia-inducible factor-1α (HIF-1α) in the gastric mucosa. Their work, published in *Digestive and Liver Disease*, identified a key pathway whereby HIF-1α, under hypoxic conditions, stabilizes and activates the tumor suppressor p53, thereby promoting apoptosis of gastric epithelial cells through modulation of the Bcl-2 family of proteins. Specifically, this involves increased expression of the pro-apoptotic protein Bax and decreased expression of the anti-apoptotic protein Bcl-2, leading to activation of cleaved caspase-3. This pathway establishes a direct link between the hemodynamic disturbances associated with portal hypertension and programmed cell death in gastric tissues.

Additional evidence regarding the role of apoptosis in intestinal injury during liver failure has been obtained from studies of acute liver failure (ALF). Song et al. (2005), in a study published in *World Journal of Gastroenterology*, demonstrated that tumor necrosis factor-alpha (TNF-α) acts as a key mediator of enterocyte apoptosis in a mouse model of ALF induced by D-galactosamine and lipopolysaccharide. They reported that the expression of tumor necrosis factor receptor 1 (TNFR1) in intestinal tissue was significantly increased and positively correlated with the level of enterocyte apoptosis measured by the TUNEL assay. This study emphasized that, in addition to the direct effects of hypoxia, circulating inflammatory cytokines—whose levels are markedly elevated in liver failure—can directly trigger apoptotic cascades in gastrointestinal epithelial cells.

Although these studies provide a strong foundation for understanding gastrointestinal injury in liver diseases, they mainly focus either on the chronic state of portal hypertension or on the acute phase of ALF. The specific and combined impact of HRS—where acute kidney injury develops on the background of chronic liver failure—on the gastric mucosa remains poorly characterized. The additional burden of renal failure introduces new pathological variables, including the accumulation of uremic toxins, metabolic acidosis, and further hemodynamic instability, all of which may exacerbate pre-existing gastric pathology. Distinguishing between apoptosis and necrosis in this context is also critically important. Apoptosis is a regulated, energy-dependent process of programmed cell death, whereas necrosis is generally a pathological and uncontrolled process resulting from excessive cellular stress and often associated with inflammation. In a clinical case reported by Takahashi et al. (2024), acute gastric mucosal necrosis was observed in a patient with short bowel syndrome and hepatorenal failure following treatment with teduglutide, highlighting the possibility of severe non-apoptotic gastric injury in the setting of multi-organ failure.

Given the above considerations, there is a clear need to investigate the morphological features of gastric mucosal injury in HRS. Understanding the relative contribution and morphological characteristics of apoptosis and necrosis may provide valuable insights into the pathogenesis of gastric complications in critically ill patients. The present study, conducted at the clinics of Tashkent State Medical University, aims to address this gap. The objective of the study is to experimentally induce HRS in a rodent model and to perform a comprehensive morphological and quantitative assessment of apoptosis and necrosis markers in the gastric mucosa using histochemical, TUNEL,

and immunohistochemical methods in order to clarify the nature and extent of epithelial cell death in the stomach under conditions of combined hepatic and renal failure.

Materials and Methods. The experimental study was conducted at the Department of Pathological Anatomy and the Central Research Laboratory of the clinics of Tashkent State Medical University.

A total of 60 adult male Wistar rats weighing 220–280 g were used. The animals were housed in standard polypropylene cages under controlled conditions (temperature 22±2°C, 12-hour light/dark cycle) with free access to standard chow and water. Before the start of the experiment, the animals were acclimatized for one week. The rats were randomly divided into three experimental groups (n = 20):

- **Sham operation (control):** midline laparotomy and manipulation of the common bile duct and liver without ligation or injection.
- **Cirrhosis (Cirr):** common bile duct ligation (BDL) to induce secondary biliary cirrhosis.
- **Hepatorenal syndrome (HRS):** BDL followed on day 21 after ligation by a single intraperitoneal injection of carbon tetrachloride (CCl_4, diluted 1:1 in olive oil, 2 ml/kg body weight) to model acute-on-chronic liver failure and provoke renal dysfunction.

Anesthesia was induced by intraperitoneal injection of ketamine (80 mg/kg) and xylazine (10 mg/kg). After a midline laparotomy, the common bile duct was isolated, double-ligated with non-absorbable silk sutures, and transected between the ligatures. The abdominal wall and skin were closed in layers with absorbable sutures. In the Sham group, the bile duct was isolated but neither ligated nor transected. Postoperatively, all animals received subcutaneous buprenorphine (0.05 mg/kg) for 48 hours for analgesia.

On day 28 after surgery (or on day 7 after CCl_4 injection for the HRS group), all animals were euthanized with an overdose of isoflurane. Blood samples were collected by cardiac puncture for serum biochemical analysis (ALT, AST, bilirubin, creatinine, and urea) to confirm the development of liver cirrhosis and HRS. The stomach was rapidly excised, opened along the greater curvature, and gently rinsed with ice-cold phosphate-buffered saline (PBS). Full-thickness samples from the gastric body were fixed in 10% neutral buffered formalin for 24 hours for histological and immunohistochemical analysis.

Morphological assessment: Formalin-fixed tissues were processed routinely, embedded in paraffin, and sectioned at a thickness of 4–5 μm. Sections were stained with hematoxylin and eosin (H&E) for general histological evaluation and detection of necrotic changes. Necrosis was identified by features such as cellular swelling (oncosis), karyolysis, cytoplasmic eosinophilia, and disruption of glandular architecture. The degree of mucosal necrosis was evaluated semi-quantitatively as follows: 0 = no necrosis; 1 = focal superficial necrosis; 2 = multifocal necrosis involving the upper third of the mucosa; 3 = confluent necrosis extending into the middle/deep mucosal layers.

Apoptosis was detected using the TUNEL (terminal deoxynucleotidyl transferase dUTP nick end labeling) assay. Deparaffinized and rehydrated sections were treated with proteinase K (20 μg/ml) for 15 min at 37°C. Endogenous peroxidase activity was blocked with 3% H_2O_2. Sections were incubated with the TUNEL reaction mixture (Roche Diagnostics, Germany) containing TdT and fluorescein-labeled dUTP for 60 min at 37°C in a humidified chamber. After washing, sections were incubated with anti-fluorescein antibody conjugated with peroxidase. The reaction was visualized using DAB, and sections were counterstained with hematoxylin. Negative controls were prepared without TdT. The apoptotic index (AI) was calculated as the percentage of TUNEL-positive epithelial cells per 1000 counted cells in 10 randomly selected non-overlapping high-power fields (HPF, 400×) per section.

Immunohistochemistry: Immunohistochemical analysis was performed to evaluate the expression of key apoptosis-related proteins: cleaved caspase-3 (pro-apoptotic executioner), Bax

(pro-apoptotic), and Bcl-2 (anti-apoptotic) using the streptavidin–biotin–peroxidase method. After deparaffinization, rehydration, and antigen retrieval (citrate buffer, pH 6.0, microwave heating for 15 min), sections were incubated overnight at 4°C with the following primary antibodies: polyclonal anti-cleaved caspase-3 (1:200, Cell Signaling), polyclonal anti-Bax (1:250, Abcam), and monoclonal anti-Bcl-2 (1:100, Dako). After washing, sections were incubated with biotinylated secondary antibodies followed by a streptavidin–peroxidase conjugate. DAB was used as the chromogen, and sections were counterstained with hematoxylin.

Immunopositivity was evaluated semi-quantitatively as the percentage of positive epithelial cells in 10 HPF. The immunoreactivity score (IRS) was calculated as the product of the percentage of positive cells (0:<5%; 1:5–25%; 2:26–50%; 3:51–75%; 4:>75%) and staining intensity (0:none; 1:weak; 2:moderate; 3:strong).

All morphological assessments were performed independently by two pathologists blinded to the experimental groups. Statistical analysis was conducted using GraphPad Prism 9.0. Data are presented as mean ± standard deviation (SD). Comparisons among multiple groups were performed using one-way ANOVA followed by Tukey's post hoc test. A value of $p<0.05$ was considered statistically significant.

Results. Serum biochemical analysis at the time of euthanasia confirmed the successful establishment of the experimental models. The BDL group demonstrated pronounced cholestasis, with significantly elevated total bilirubin, ALT, and AST levels compared with the Sham group ($p<0.01$). The HRS group (CCl_4 administration on the background of cirrhosis) showed a further significant increase in liver enzymes and, importantly, a marked elevation in serum creatinine and urea levels compared with both the Sham and Cirrhosis groups ($p<0.01$ vs. Cirr), confirming the development of acute renal failure on the background of chronic liver disease.

Histological examination of the gastric mucosa revealed clear differences among the groups:

- **Sham:** Normal histological structure. The surface epithelium was intact, and gastric pits and glands were well organized. No signs of inflammatory infiltration, edema, or cell death were observed (Fig. 1A).
- **Cirr:** Features consistent with portal hypertensive gastropathy. There was pronounced submucosal vascular congestion and dilation. The mucosa showed areas of interstitial edema and a moderate increase in inflammatory cells. Foci of epithelial damage with pyknotic nuclei and condensed cytoplasm were observed, indicating apoptosis. Foci of coagulative necrosis were rare—observed in only 20% (4/20) of samples—and were limited to the superficial epithelium.
- **HRS:** The most severe and extensive injury was observed in this group. In addition to vascular congestion, widespread destruction of the mucosal architecture was noted. Foci of coagulative necrosis were present in 75% (15/20) of samples ($p<0.001$ vs. Cirr). These lesions were characterized by sheets of epithelial cells with eosinophilic cytoplasm, karyorrhexis, and karyolysis, along with loss of normal glandular structure, frequently extending into the middle third of the mucosa (Fig. 1B). Marked edema, hemorrhage, and mixed inflammatory infiltrates were also observed in the surrounding tissue.

The TUNEL assay was used to quantitatively assess apoptosis. TUNEL-positive cells were identified by the characteristic brown nuclear staining.

- **Sham:** Only occasional TUNEL-positive cells were observed, reflecting the normal low level of epithelial turnover (Fig. 1C).

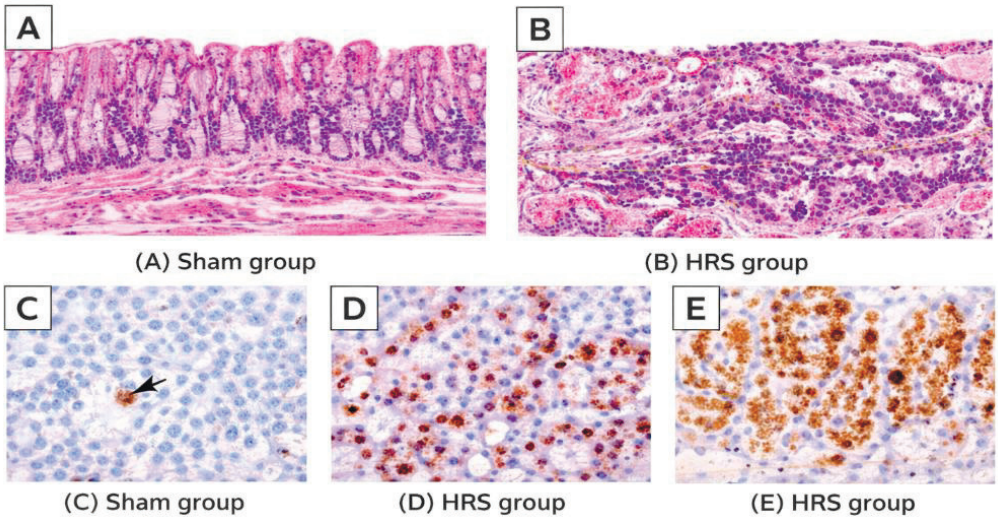


Fig. 1. Morphological and Immunohistochemical Analysis of the Gastric Mucosa

(A) Sham group: normal gastric mucosa (H&E, 200×).(B) HRS group: focus of coagulative necrosis with loss of glandular architecture and inflammatory infiltration (H&E, 200×).(C) Sham group: rare TUNEL-positive cells (arrow) (TUNEL, 400×).(D) HRS group: numerous TUNEL-positive apoptotic cells (brown nuclei) throughout the gastric mucosa (TUNEL, 400×).(E) HRS group: strong cytoplasmic immunostaining for cleaved caspase-3 in epithelial cells (IHC, 400×).

Cirrhosis group: In the cirrhosis group, a significant increase in the number of apoptotic cells was observed, predominantly located in the upper third of the gastric glands. The apoptotic index (AI) increased markedly to 18.5±3.4%**,** which was significantly higher than in the Sham group ($p<0.01$).

HRS group: The highest frequency of apoptosis was observed in the HRS group**.** TUNEL-positive cells were numerous and distributed throughout the full thickness of the mucosa. The AI in the HRS group reached 34.7±5.2%**,** which was significantly higher than in both the Sham and cirrhosis groups ($p<0.01$ vs. both groups) (Fig. 1D).

Immunohistochemistry**.** Bax and Bcl-2 expression: In the Sham group**,** the expression of the pro-apoptotic protein Bax was minimal, whereas the anti-apoptotic protein Bcl-2 showed moderate expression, resulting in a low Bax/Bcl-2 ratio (0.22) favoring cell survival. In the cirrhosis group, a significant shift was observed: Bax expression increased markedly while Bcl-2 expression decreased, leading to an increased Bax/Bcl-2 ratio of 1.38. The most pronounced pro-apoptotic shift was found in the HRS group, characterized by intense and widespread Bax expression together with weak, focal Bcl-2 expression, resulting in a Bax/Bcl-2 ratio of 4.67.

Cleaved caspase-3 expression: Cleaved caspase-3, an active executioner caspase, was used as a reliable marker of apoptosis. Its expression closely corresponded to the apoptotic index. In the Sham group, positive cells were rarely observed. In the cirrhosis group, a significant increase was noted (IRS 5.8±1.5). The highest expression was observed in the HRS group, characterized by strong cytoplasmic staining in numerous epithelial cells, particularly in regions adjacent to—but distinct from—necrotic foci (IRS 11.2±2.1, $p<0.01$ vs. Cirr) (Fig. 1E).

The simultaneous presence of foci of coagulative necrosis and a high apoptotic index in the HRS group indicates a mixed pattern of cell death. The gastric mucosa in HRS is subjected to such severe injury that both the regulated apoptotic pathway and the uncontrolled necrotic pathway are activated simultaneously.

Discussion. The results provide a detailed morphological characterization of gastric mucosal injury in an experimental model of hepatorenal syndrome. The damage observed in the HRS group was substantially more severe and qualitatively different from the changes seen in cirrhosis alone. The principal finding of this study is that the superimposition of acute renal failure on chronic liver disease creates a pathophysiological environment that induces both apoptosis and necrosis of gastric epithelial cells.

In the cirrhosis group, the findings are consistent with previously reported features of portal hypertensive gastropathy, including an increased apoptotic index and a shift in the Bax/Bcl-2 ratio toward apoptosis. Histologically, vascular congestion and mucosal edema—typical features of portal hypertension—were observed. However, the injury was largely limited to apoptosis, while necrotic changes were rare and superficial.

In contrast, the transition to the HRS group demonstrates a critical aggravation of mucosal injury. The marked elevation of creatinine and urea confirms the development of renal failure, which further exacerbates the existing hepatic dysfunction. The accumulation of uremic toxins**,** metabolic acidosis, and hemodynamic instability intensifies mucosal hypoperfusion. This leads to severe cellular energy depletion and a shift from apoptosis to necrosis, reflected by the presence of coagulative necrosis in 75% of samples. Despite this, a high level of apoptosis persists, as demonstrated by TUNEL positivity and increased cleaved caspase-3 expression. The markedly elevated Bax/Bcl-2 ratio (4.67) indicates activation of the intrinsic (mitochondrial) apoptotic pathway. The enhanced apoptotic activity likely results from a combination of chronic hypoxia (HIF-1α/p53 signaling) and systemic inflammatory and uremic toxicity (TNF-α), which may further activate the extrinsic apoptotic pathway.

The coexistence of apoptosis and necrosis in the HRS group suggests a necrosis–apoptosis continuum, in which cells that initially activate apoptotic pathways may ultimately undergo necrotic death under conditions of severe ATP depletion. This phenomenon has important clinical implications: apoptosis is generally a silent process, whereas necrosis provokes inflammation, disrupts the mucosal barrier, and significantly increases the risk of gastrointestinal bleeding.

Conclusion. This experimental study conducted at the clinics of Tashkent State Medical University demonstrates that hepatorenal syndrome significantly aggravates gastric mucosal injury compared with cirrhosis alone. The gastric mucosa is characterized by a mixed pattern of cell death, including markedly increased apoptosis (reflected by the Bax/Bcl-2 shift and caspase-3 activation) together with extensive foci of coagulative necrosis. These findings highlight that the gastric mucosa represents an important target organ in HRS and may partly explain the high risk of gastrointestinal bleeding in such patients. Therapeutic strategies for HRS should therefore consider protection of the gastric mucosal barrier alongside correction of hepatic and renal dysfunction.

REFERENCES

1. Gines, P., Krag, A., Abraldes, J. G., Sola, E., Fabrellas, N., & Kamath, P. S. (2021). Liver cirrhosis. The Lancet, 398(10308), 1359–1376.

2. Kamath, P. S., Lacerda, M., Ahlquist, D. A., McKusick, M. A., Andrews, J. C., & Nagorney, D. A. (2000). Gastric mucosal responses to intrahepatic portosystemic shunting in patients with cirrhosis. Gastroenterology, 118(5), 905–911.

3. Moll, U. M., & Zaika, A. (2001). Nuclear and mitochondrial apoptotic pathways of p53. FEBS Letters, 493(2–3), 65–69.

4. Nazarova, M. B., Adilbekova, D. B., Akhrorov, A. A., Toshpulatov, S. S., & Rustamova, F. O. (2025). The morphological and morphometrical state of the liver's in offspring born to mothers with chronic toxic hepatitis under conditions of medication correction before pregnancy (experimental study). Central Asian Journal of Medicine, eISSN: 2181-1326, 77–84.

5. Nazarova, M. B., Adilbekova, D. B., Akhrorov, A. A., Toshpulatov, S. S., & Rustamova, F. O. (2025). The morphological and morphometric state of the liver's vascular tissue structures in the offspring of intact experimental rats during postnatal ontogeny dynamics (experimental study). Central Asian Journal of Medicine, eISSN: 2181-1326, 50–57.

6. Ohta, M., Yamaguchi, S., Gotoh, N., & Tomikawa, M. (2002). Pathogenesis of portal hypertensive gastropathy: a clinical and experimental review. Surgery, 131(1), S165–S170.

7. Rockey, D. C. (2019). An update: portal hypertensive gastropathy and colopathy. Clinics in Liver Disease, 23(4), 643–658.

8. Song, H. L., Lu, S., & Liu, P. (2005). Tumor necrosis factor-alpha induces apoptosis of enterocytes in mice with fulminant hepatic failure. World Journal of Gastroenterology, 11(24), 3701–3709.

9. Takahashi, T., Maejima, T., Miyazaki, D., Fukahori, S., & Hagiwara, M. (2024). Teduglutide-induced acute gastric mucosal necrosis in short bowel syndrome with hepatorenal failure: Case report. International Journal of Surgery Case Reports, 117, 109524.

10. Tan, S., Li, L., Chen, T., Chen, X., Tao, L., Lin, X., … & Wu, B. (2015). β-Arrestin-1 protects against endoplasmic reticulum stress/p53-upregulated modulator of apoptosis-mediated apoptosis via repressing p-p65/inducible nitric oxide synthase in portal hypertensive gastropathy. Free Radical Biology and Medicine, 87, 69–83.

11. Wang, G. L., Jiang, B. H., Rue, E. A., & Semenza, G. L. (1995). Purification and characterization of hypoxia-inducible factor 1. Journal of Biological Chemistry, 270(3), 1230–1237.

12. Zhang, Y., Lu, H., Ji, H., & Li, Y. (2023). p53 upregulated by HIF-1α promotes gastric mucosal epithelial cells apoptosis in portal hypertensive gastropathy. Digestive and Liver Disease, 55(1), 81–92.